JACS
JOURNAL OF THE AMERICAN CHEMICAL SOCIETY
Communication
pubs.acs.org/JACS

A Facile Approach for Controlling the Orientation of One-Dimensional Mesochannels in Mesoporous Titania Films

Feng Shan,[†] Xuemin Lu,*[,†] Qian Zhang,[†] Jun Wu,[†] Yuzhu Wang,[‡] Fenggang Bian,[‡] Qinghua Lu,*[,†] Zhaofu Fei,[§] and Paul J. Dyson[§]

[†]School of Chemistry and Chemical Engineering, the State Key Laboratory of Metal Matrix Composites, Shanghai Jiao Tong University, Shanghai 200240, P.R. China

[‡]Shanghai Synchrotron Radiation Facility, Shanghai Institute of Applied Physics, Chinese Academy of Sciences, Shanghai 200240, P.R. China

[§]Institut des Sciences et Ingénierie Chimiques, Ecole Polytechnique Fédérale de Lausamne (EPFL), CH-1015, Lausanne, Switzerland

Supporting Information

ABSTRACT: Controlling of the orientation of mesochannels in mesostructured thin films is important for the development of novel molecular devices and, in particular, generating vertically aligned mesochannels with respect to the substrate plane is extremely challenging for nonsiliceous materials. We describe a facile and highly effective air flow method, which is able to control the unidirectional alignment of titania mesochannels in a desired direction (e.g., parallel, perpendicular, or oblique) on a large scale, via manipulation of the air flow rate and incident angle. The titania mesochannels were characterized by TEM, SEM, SAXRD, and GISAXS. The unidirectional, vertically aligned mesostructured titania films were found to exhibit excellent ion conductivity.

Polymer-templated mesostructured organic/inorganic hybrid materials and their corresponding calcined mesoporous derivatives provide a route to prepare a large range of mesostructures with tailor-made properties.[1] The fine control of one-dimensional (1D) channels of such mesomaterials in a certain direction is of considerable interest due to the demand for novel molecular-scale devices.[2] Previous attempts have been made to develop mesostructured films with uniform pore orientation, and the alignment of mesochannels parallel to the substrate surface has been achieved with silica films using external fields[3] and anisotropic surfaces,[4] thereby affording materials with macroscopically anisotropic properties.[5] Compared to parallel mesochannels in mesoporous films, vertical alignment of mesochannels with respect to the surface is much more difficult to achieve, although highly desirable, because such ordered mesoporous structures can provide transmission channels for electrons, ions, and fluids, which are especially suited to solar cells, fuel cells, separation technologies, etc.[6] In spite of intensive efforts, only a few examples describing the preparation of vertically aligned mesochannels have been reported. Magnetic fields of the order of 10−30 T[3c,7] and confinement in anodized alumina channels[6b] have been used to generate vertical channels in mesoporous thin films, but these methods are limited to small areas. Mesoscale epitaxial-like growth may be used to obtain vertical alignment of channels,[6d,8] but alignment over an entire surface has not been achieved. Vertical channels were obtained in silica films via cathodic electrodeposition; however, the thickness of the ordered mesoporous film is limited to the range 40−150 nm.[3e] Moreover, most of these pioneering studies have focused on silica frameworks.

In an excellent and recent review on mesoporous films the major challenges in this field were identified, which include the precise control of 1D mesochannels in any direction and the realization of well-ordered alignments of mesoporous thin films based on materials other than silica.[2b,9] In this contribution we describe a simple and effective method that addresses these two major challenges, thus allowing the preparation of uniaxially oriented mesoporous titania films in any uniaxial alignment direction via the manipulation of the magnitude and incident direction of a shear-force in a hot-air flow. This approach builds on our previous work in which silica mesochannels oriented in parallel were obtained.[3f]

To precisely control the orientation of the mesopores in the film two parameters need to be controlled, the incident angle of the air jet with respect to the surface plane and the rate of solvent evaporation, the latter is determined by the temperature and the air flow rate. To demonstrate the approach, drops of a titania sol precursor were pipetted directly onto a clean silicon wafer to form a liquid film, and then a jet of hot air at a constant temperature of 70 °C was applied over the substrate surface for 10 s (the air flow speed was varied from 9.5−5.5 m/s, and the incident angle α was varied from 0−70°; α refers to the incident angle subtended between the substrate plane and the incident air flow), followed by aging at 20 °C for 24 h under a controlled humidity of ∼70−80%. On the basis of comparisons to literature data,[10] the obtained titania films were shown to comprise 2D hexagonal mesophase (*p6mm*). Transmission electron microscopy (TEM) of the powders scraped off the films and small-angle X-ray diffraction (SAXRD) of films annealed at 200 °C further confirm the 2D hexagonal structure (Figure 1), with a lattice spacing of d = 9.4 nm.

Examination of these films by cross-sectional TEM revealed that the gas flow rate effectively controls the alignment of the

Received: September 15, 2012
Published: December 5, 2012

dx.doi.org/10.1021/ja309168f | J. Am. Chem. Soc. 2012, 134, 20238−20241

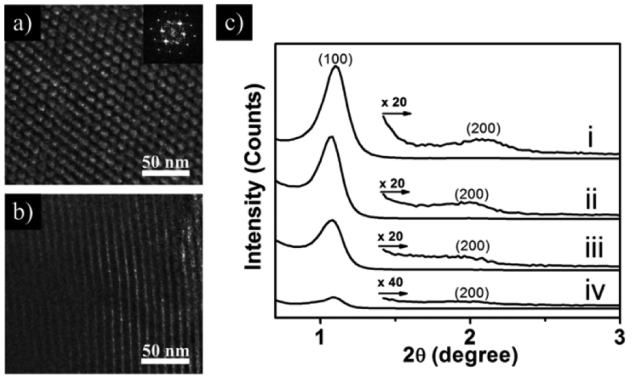

Figure 1. (a and b) TEM images of titania powder removed from a mesostructured film prepared by horizontal air flow at the speed of 9.5 m s^{-1}. Inset in (a) corresponds to the fast-Fourier-transform (FFT) diffractogram. (c) Small-angle XRD patterns of mesostructured titania films. Mesostructured films were synthesized with air flows of 5.5 m/s at various incident angles of (i) 0°, (ii) 20°, (iii) 40°, and (iv) 50°.

titania mesochannels (a–c of Figure 2). The resulting titania films obtained at high air-flow rates of 9.5 and 8 m/s exhibit uniaxially ordered mesostructures with mesochannels parallel to the air-flow direction over the entire thickness (Figure 2a and b). Decreasing the air flow rate led to the formation of obliquely ordered mesochannels, although the shear force was still parallel to the substrate (α = 0°). Large-domain periodically oblique mesochannels tilted by ~40° with respect to the wafer surface (Figure 2c) were obtained at an air flow rate of 5.5 m/s.

As the incident angle of the gas is varied from 0 to 50°, the mesochannel tilt angle increases from 40° to nearly 90° at an airspeed of 5.5 m/s, hence affording a perpendicularly aligned mesostructured titania film. The cross-sectional SEM image and its top-view image corresponding to the sample in Figure 2e are provided in the Supporting Information (SI) and are consistent with the orientation observed in the TEM image; see Figure S1 in the SI. SAXRD was used to estimate the direction of the channels in the mesoporous films since the technique is sensitive only to periodic structure parallel to the substrate.[3c,11] The structural information provided by the SAXRD profiles (Figure 1c) is consistent with the cross-sectional TEM data. As the incident angle of air flow is increased from 0° to 50°, the diffraction intensity of the corresponding mesoporous film gradually decreases until no peak is observed in the profile, indicative of perpendicular oriented mesochannels. The relationship between the mesochannel orientation and the incident angle and flow rate of the air is summarized in Table S1 (SI). The flow rate and the incident angle of the air flow appear to be the key factors that control the orientation of the mesochannels. At lower air flow rates the mesochannel orientation is dependent on the incident direction of air flow, whereas at higher air flows there is a deterioration of the mesochannel orientation.

Grazing-incidence small-angle X-ray scattering (GISAXS) analysis was further carried out in order to confirm the macroscopic information concerning the alignment of mesochannels (Figure 3). For the parallel oriented films, the GISAXS pattern comprises three diffraction spots that may be attributed to (01) and (10) planes that were found (Figure 3a), providing further evidence that the mesochannels are arranged in a hexagonal phase; this conclusion is also supported by the fact that the scattering peaks in the GISAXS pattern have a q^* ratio of 1: $\sqrt{3}$:$\sqrt{4}$:$\sqrt{7}$ (see Figure S2 in SI). Rotation of the sample by 90° results in the disappearance of the two in-plane (10) spots (Figure 3b) and the anisotropy of the diffraction patterns indicates that the cylindrical mesochannels are aligned parallel to the direction of air flow.[4c,12] In addition, weak background rings are observed in a and b of Figure 3, indicating that a few wormlike mesochannels may exist in the films. Figure 3c shows the patterns of the vertically oriented film, recorded with the incident X-rays parallel to the direction of the applied flux. The two in-plane (10) spots are observed to the left and right of the beam, and there is no diffracted intensity out of the plane of the film (01). A similar pattern is observed when the incident direction of the X-ray beam is perpendicular to the

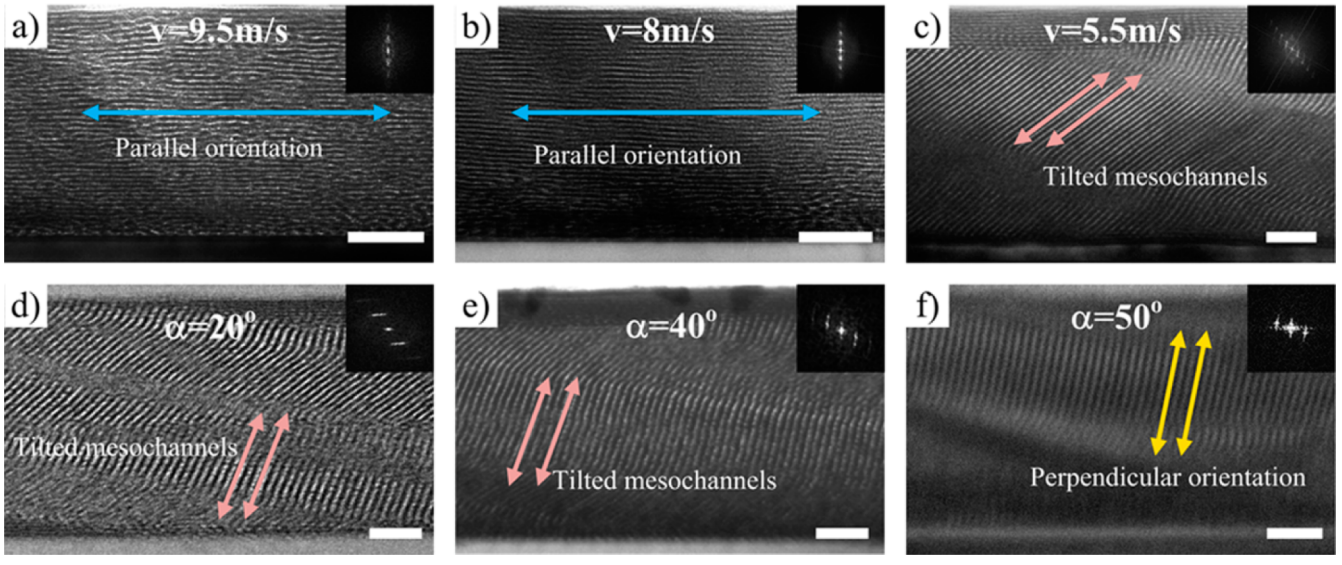

Figure 2. Effect of air flow rate and incident angle on mesochannel alignment. (a–c) Cross-sectional TEM images of mesostructured titania films deposited on silicon substrates with horizontal air flow rates of (a) 9.5 m/s, (b) 8 m/s, and (c) 5.5 m/s. (d–f) Cross-sectional TEM images of the mesostructured titania films grown on silicon wafers with air flow incident angles of (d) 20°, (e) 40°, and (f) 50° at a flow rate of 5.5 m/s. The insets correspond to the FFT diffractograms. All samples were sliced along the air-flow direction with the air flowing from right to left. Scale bar = 100 nm.

dx.doi.org/10.1021/ja309168f | J. Am. Chem. Soc. 2012, 134, 20238–20241

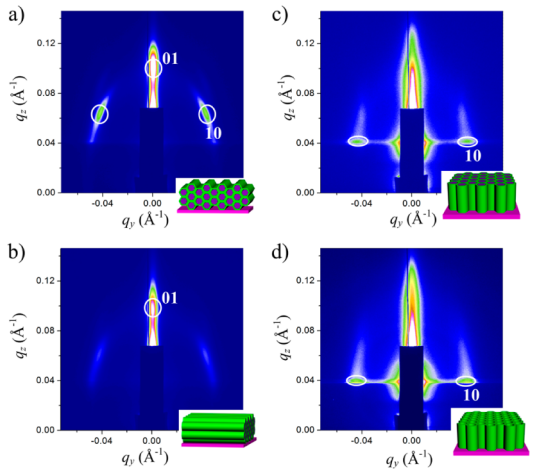

Figure 3. GISAXS patterns of mesostructured titania films heat-treated at 200 °C: (a and b) sample oriented in parallel; (c) vertically aligned sample; (d) vertically aligned sample calcined at 350 °C. [(a, c, d) Samples were measured with the incident X-rays parallel to the direction of air-flow.] (b) Sample "a" was rotated by 90°.

direction of the applied air flow (see Figure S3 in SI). Combined, these data show that the titania mesochannels are oriented perpendicular to the substrate surface.[8,13] In order to investigate the effect of thermal treatment on the phase structure of the obtained titania film, the mesostructured film was also analyzed by GISAXS after removal of the surfactant by calcination, see Figure 3d. Similar patterns are observed, indicating that the initial structure is maintained and no morphological transformations occur following calcination at 350 °C for 3 h (Figure 3d and Figure S3 [SI]). In addition, besides silicon wafer, we also have succeeded in controlling the titania mesochannel orientation on glass slide, fluorine-doped tin oxide (FTO) substrate and metal substrate, indicating that substrate surface does not affect the orientation at the interface region.

It is not unreasonable to assume that the mesochannel growth mechanism presumably involves the initial formation of cylindrical micelle templates assembled from the surfactants following solvent evaporation under the shear force generated by the air flow. After depositing the titania sol onto the substrate surface, the precursor solution is homogeneous; upon application of the hot gas the sol is dispersed along the substrate, and the solvent immediately starts to evaporate. This process results in a concentration gradient with the highest surfactant concentration at the solution surface, and cylindrical micelles form at the liquid–vapor interface (Scheme 1). The orientation of these cylindrical micelles is simultaneously affected by the shear force generated by the flow of air and the upward growth induced by solvent evaporation. Accordingly, the cylinders are aligned along the direction of the resultant force. Following removal of the incident air flow, the residual butanol continues to evaporate at a high rate as the sol remains hot. Evaporation of solvent provides a strong, highly directional field,[14] which in this case results in the formation of perpendicular mesochannels. In this process, the shear force from the air flow is a significant prerequisite as the vertically ordered mesochannels do not form if solvent evaporation occurs in the absence of a hot air flow (see Figure S4 in SI). This tentative mechanism not only explains how vertically aligned mesochannels can be prepared in an inclined air flow

Scheme 1. Illustration of the Process Used To Generate the Vertically Aligned Mesochannels

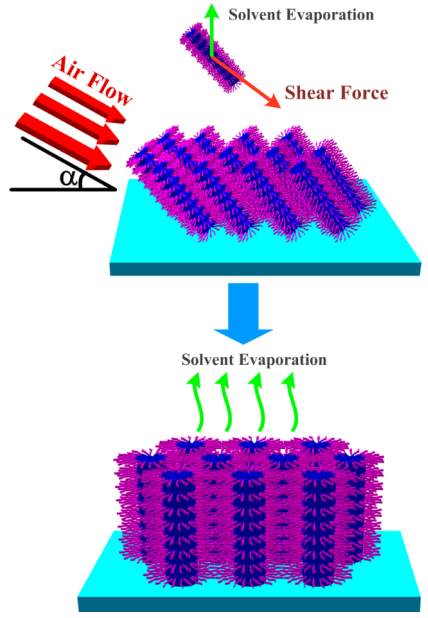

but also accounts for the mesochannel tilt angle always being wider than the air flow incident angle.

Under a stronger shear force, the mesochannel orientation is predominantly controlled by the shear-induced orientation, and the channels align along the direction of the incident air-flow (a and b of Figure 2). At increased air flow rates evaporation is considerably faster, leading to an increase in the randomness of the mesopore orientation and the formation of randomly oriented worm-like mesochannels (see Figure S5 in SI).

The electrochemical properties of the mesoporous titania films were determined by coverage studies of a FTO electrode coated with the film in order to ascertain the influence of ion conductivity of the film as a function of the channel orientation. Figure 4 displays the cyclic voltammograms of the electrode-supported mesostructured titania films ordered vertically and in parallel in the presence of $[Fe(CN)_6]^{3-}$ (1 mM). Before calcination, no electrochemical response to the solution-phase redox probe $K_3Fe(CN)_6$ could be observed (Figure 4e). The

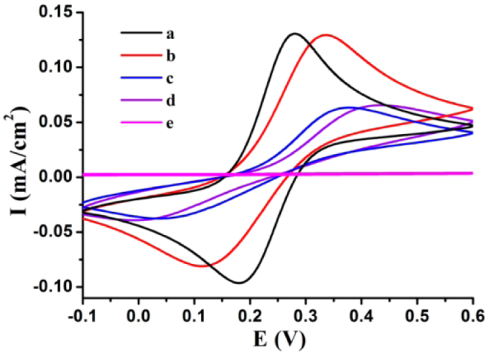

Figure 4. Electrochemical monitoring of the permeability properties of the mesostructured films. Cyclic voltammograms of $Fe(CN)_6^{3-}$/$Fe(CN)_6^{4-}$ on (a) a bare FTO electrode, (b) vertically oriented, (c) oriented in parallel, (d) randomly oriented mesoporous titania films, and (e) vertically oriented mesostructured titania film prior to removal of the surfactant.

dx.doi.org/10.1021/ja309168f | J. Am. Chem. Soc. 2012, 134, 20238–20241

film was completely closed to any external reagent, indicating that mesostructured titania homogeneously coated the entire electrode surface. After removal of the residual template from the mesochannels by calcination at 350 °C a well-defined electrochemical response of the $Fe(CN)_6^{3-}$ ions was observed (Figure 4b), demonstrating effective charged molecular transport across the template-free mesoporous titania. As expected, the peak current measured with vertically oriented mesochannels was significantly higher than that measured with parallel oriented or randomly oriented mesochannels, being almost the same as that of a bare FTO electrode.

In conclusion, we have developed an air flow method to control the growth of 1D mesochannels in mesoporous titania films. By simply regulating the rate and incident angle of the air flow, the orientation of the mesochannels can be controlled, thus affording parallel, vertical, and oblique orientations, with any angle with respect to the plane. Importantly, the method is suitable for the large-scale preparation of films. The macroscopically vertically ordered mesoporous titania film was found to efficiently conduct ions, and consequently, such titania films have considerable potential in light-harvesting devices such as dye-sensitized and quantum dot solar cells.

■ ASSOCIATED CONTENT

Supporting Information

Experimental details for the preparation of the films, full details of the GISAXS data, TEM and SEM images, and film characteristics. This material is available free of charge via the Internet at http://pubs.acs.org.

■ AUTHOR INFORMATION

Corresponding Author

xueminlu@sjtu.edu.cn (X. L.); qhlu@sjtu.edu.cn (Q. L.).

Notes

The authors declare no competing financial interest.

■ ACKNOWLEDGMENTS

This work was supported by the National Science Fund for Distinguished Young Scholars (50925310), the National Science Foundation of China (50902094,51173103), 973 Project (2009CB93043, 2012CB933803), and excellent academic leaders of Shanghai (11XD1403000).

■ REFERENCES

(1) (a) Yang, P.; Wirnsberger, G.; Huang, H. C.; Cordero, S. R.; McGehee, M. D.; Scott, B.; Deng, T.; Whitesides, G. M.; Chmelka, B. F.; Buratto, S. K.; Stucky, G. D. *Science* **2000**, *287*, 465. (b) Antonelli, D. M.; Ying, J. Y. *Angew. Chem., Int. Ed. Engl.* **1995**, *34*, 2014. (c) Alberius, P. C. A.; Frindell, K. L.; Hayward, R. C.; Kramer, E. J.; Stucky, G. D.; Chmelka, B. F. *Chem. Mater.* **2002**, *14*, 3284. (d) Crepaldi, E. L.; Soler-Illia, G.; Grosso, D.; Cagnol, F.; Ribot, F.; Sanchez, C. *J. Am. Chem. Soc.* **2003**, *125*, 9770. (e) Fan, R.; Karnik, R.; Yue, M.; Li, D.; Majumdar, A.; Yang, P. *Nano Lett.* **2005**, *5*, 1633. (f) Maex, K.; Baklanov, M. R.; Shamiryan, D.; Iacopi, F.; Brongersma, S. H.; Yanovitskaya, Z. S. *J. Appl. Phys.* **2003**, *93*, 8793. (g) Martini, I. B.; Craig, I. M.; Molenkamp, W. C.; Miyata, H.; Tolbert, S. H.; Schwartz, B. J. *Nat. Nanotechnol.* **2007**, *2*, 647.

(2) (a) Miyata, H.; Kuroda, K. *J. Am. Chem. Soc.* **1999**, *121*, 7618. (b) Wu, K. C.-W.; Jiang, X.; Yamauchi, Y. *J. Mater. Chem.* **2011**, *21*, 8934.

(3) (a) Hillhouse, H. W.; Okubo, T.; van Egmond, J. W.; Tsapatsis, M. *Chem. Mater.* **1997**, *9*, 1505. (b) Tolbert, S. H.; Firouzi, A.; Stucky, G. D.; Chmelka, B. F. *Science* **1997**, *278*, 264. (c) Yamauchi, Y.; Sawada, M.; Noma, T.; Ito, H.; Furumi, S.; Sakka, Y.; Kuroda, K. *J. Mater. Chem.* **2005**, *15*, 1137. (d) Melosh, N. A.; Davidson, P.; Feng, P.; Pine, D. J.; Chmelka, B. F. *J. Am. Chem. Soc.* **2001**, *123*, 1240. (e) Walcarius, A.; Sibottier, E.; Etienne, M.; Ghanbaja, J. *Nat. Mater.* **2007**, *6*, 602. (f) Su, B.; Lu, X..; Lu, Q. *J. Am. Chem. Soc.* **2008**, *130*, 14356.

(4) (a) Miyata, H.; Kuroda, K. *Chem. Mater.* **1999**, *11*, 1609. (b) Su, B.; Lu, X.; Lu, Q. *Langmuir* **2008**, *24*, 9695. (c) Radhakrishnan, L.; Wang, H.; Yamauchi, Y. *Chem.—Asian. J.* **2010**, *5*, 1290.

(5) (a) Fukuoka, A.; Miyata, H.; Kuroda, K. *Chem. Commun.* **2003**, 284. (b) Molenkamp, W. C.; Watanabe, M.; Miyata, H.; Tolbert, S. H. *J. Am. Chem. Soc.* **2004**, *126*, 4476. (c) Shan, F.; Lu, X.; Zhang, Q.; Su, B.; Lu, Q. *Langmuir* **2012**, *28*, 812.

(6) (a) Weng, W.; Higuchi, T.; Suzuki, M.; Fukuoka, T.; Shimomura, T.; Ono, M.; Radhakrishnan, L.; Wang, H. J.; Suzuki, N.; Oveisi, H.; Yamauchi, Y. *Angew. Chem., Int. Ed.* **2010**, *49*, 3956. (b) Yamaguchi, A.; Uejo, F.; Yoda, T.; Uchida, T.; Tanamura, Y.; Yamashita, T.; Teramae, N. *Nat. Mater.* **2004**, *3*, 337. (c) Tominaka, S.; Wu, C.-W.; Momma, T.; Kuroda, K.; Osaka, T. *Chem. Commun.* **2008**, 2888. (d) Hara, M.; Nagano, S.; Seki, T. *J. Am. Chem. Soc.* **2010**, *132*, 13654.

(7) (a) Yamauchi, Y.; Sawada, M.; Sugiyama, A.; Osaka, T.; Sakka, Y.; Kuroda, K. *J. Mater. Chem.* **2006**, *16*, 3693. (b) Yamauchi, Y.; Sawada, M.; Komatsu, M.; Sugiyama, A.; Osaka, T.; Hirota, N.; Sakka, Y.; Kuroda, K. *Chem.—Asian. J.* **2007**, *2*, 1505.

(8) Richman, E. K.; Brezesinski, T.; Tolbert, S. H. *Nat. Mater.* **2008**, *7*, 712.

(9) Oveisi, H.; Jiang, X.; Imura, M.; Nemoto, Y.; Sakamoto, Y.; Yamauchi, Y. *Angew. Chem., Int. Ed.* **2011**, *50*, 7410.

(10) Choi, S. Y.; Mamak, M.; Coombs, N.; Chopra, N.; Ozin, G. A. *Adv. Funct. Mater.* **2004**, *14*, 335.

(11) Hillhouse, H. W.; van Egmond, J. W.; Tsapatsis, M.; Hanson, J. C.; Larese, J. Z. *Microporous Mesoporous Mater.* **2001**, *44*, 639.

(12) Miyata, H.; Kubo, W.; Sakai, A.; Ishida, Y.; Noma, T.; Watanabe, M.; Bendavid, A.; Martin, P. J. *J. Am. Chem. Soc.* **2010**, *132*, 9414.

(13) (a) Koganti, V. R.; Dunphy, D.; Gowrishankar, V.; McGehee, M. D.; Li, X.; Wang, J.; Rankin, S. E. *Nano Lett.* **2006**, *6*, 2567. (b) Ma, C.; Han, L.; Jiang, Z.; Huang, Z.; Feng, J.; Yao, Y.; Che, S. *Chem. Mater.* **2011**, *23*, 3583. (c) Teng, Z.; Zheng, G.; Dou, Y.; Li, W.; Mou, C.-Y.; Zhang, X.; Asiri, A. M.; Zhao, D. *Angew. Chem., Int. Ed.* **2012**, *51*, 2173.

(14) (a) Lin, Z. Q.; Kim, D. H.; Wu, X. D.; Boosahda, L.; Stone, D.; LaRose, L.; Russell, T. P. *Adv. Mater.* **2002**, *14*, 1373. (b) Kim, S. H.; Misner, M. J.; Xu, T.; Kimura, M.; Russell, T. P. *Adv. Mater.* **2004**, *16*, 226.